Atmos. Chem. Phys. Discuss., https://doi.org/10.5194/acp-2018-21
Manuscript under review for journal Atmos. Chem. Phys.
Discussion started: 31 January 2018

Atmospheric Chemistry and Physics Discussions

Ice crystal number concentration estimates from lidar-radar satellite retrievals. Part 2: Controls on the ice crystal number concentration

Edward Gryspeerdt[1], Odran Sourdeval[2], Johannes Quaas[2], Julien Delanoë[3], and Philipp Kühne[2]

[1]Space and Atmospheric Physics Group, Imperial College London, London, United Kingdom
[2]Institute for Meteorology, Universität Leipzig, Germany
[3]Laboratoire Atmosphères, Milieux, Observations Spatiales/IPSL/UVSQ/CNRS/UPMC, Guyancourt, France

Correspondence: Edward Gryspeerdt
(e.gryspeerdt@imperial.ac.uk)

Abstract. The ice crystal number concentration (N_i) is a key property of ice clouds, both radiatively and microphysically. However, due to sparse in-situ measurements of ice cloud properties, the controls on the N_i have remained difficult to determine. As more advanced treatments of ice clouds are included in global models, it is becoming increasingly necessary to develop strong observational constraints on the processes involved.

This work uses the DARDAR-LIM N_i retrieval described in part one to investigate the controls of the N_i at a global scale. The retrieved clouds are separated by type. The effects of temperature, proxies for in-cloud updraught and aerosol concentrations are investigated. Variations in the cloud top N_i ($N_{i(top)}$) consistent with both homogeneous and heterogeneous nucleation are observed and along with a possible role of aerosol both increasing and decreasing the $N_{i(top)}$ depending on the prevailing meteorological situation. Away from the cloud top, the N_i displays a different sensitivity to these controlling factors, providing a possible explanation to the low N_i sensitivity to temperature and INP observed in previous in-situ studies.

This satellite dataset provides a new way of investigating the response of cloud properties to meteorological and aerosol controls. The results presented in this work increase our confidence in the retrieved N_i and will form the basis for further study into the processes influencing ice and mixed phase clouds.

1 Introduction

Clouds play a central role in the Earth's energy budget, being responsible for large variations in the reflected shortwave and emitted longwave radiation (Stephens et al., 2012). The response of clouds to changing greenhouse gases and aerosols remains one of the largest uncertainties in understanding past and future climate changes (Boucher et al., 2013). Significant advances (eg. Quaas et al., 2009; Seifert et al., 2015; Gryspeerdt et al., 2016) have been made into modelling and observing the role of aerosols in liquid clouds, but the impact of aerosols on high clouds remains uncertain (Heyn et al., 2017). A large part of this uncertainty comes from the difficulty in retrieving cirrus cloud properties at a large enough scale to separate the roles of individual factors controlling the ice crystal number concentration (N_i).

Atmos. Chem. Phys. Discuss., https://doi.org/10.5194/acp-2018-21
Manuscript under review for journal Atmos. Chem. Phys.
Discussion started: 31 January 2018

Atmospheric Chemistry and Physics Discussions

A key microphysical property of ice clouds, the N_i links the aerosol environment to dynamic effects driving cloud updraughts and the generation of supersaturation (Pruppacher and Klett, 1997). Through changes in the ice crystal size, changes in the N_i can have far-reaching implications for a cloud, impacting the radiative (Liou, 1986; Fusina et al., 2007), precipitation and cloud lifetime properties (Lindsey and Fromm, 2008). Given the importance of the N_i, it is often used as a prognostic variable in two moment cloud microphysics schemes (e.g. Lohmann et al., 2007; Salzmann et al., 2010). This highlights a requirement to understand the controls on the N_i for improving our understanding and parametrisation of cloud processes. While aircraft measurements of the N_i exist, they are restricted in space and time. They can be affected by shattering of ice crystals at the instrument inlet (Korolev et al., 2013) and difficulties in measuring the smallest crystals (O'Shea et al., 2016). In this paper, the new DARDAR-LIM satellite dataset described in part one (Sourdeval et al., submitted) allows the processes that control the N_i to be investigated globally.

It is known that the temperature plays a strong role in determining the ice crystal nucleation rate. The homogeneous nucleation rate is a strong function of temperature (Koop et al., 2000), with atmospherically relevant nucleation only taking place at temperatures colder than 235 K. This strong temperature dependence in the nucleation rate does not necessarily correspond to a strong temperature dependence in the N_i (Heymsfield and Miloshevich, 1993). A weak N_i temperature dependence was found by Gayet et al. (2004). Krämer et al. (2009) found similar results, with a slight reduction in the N_i for the coldest measurements. Using a different dataset, Muhlbauer et al. (2014) showed an increase in N_i with decreasing temperature, concentrating primarily on synoptic and frontal cirrus.

The in-situ homogeneous nucleation of ice crystals is also dependent on the supersaturation (Koop et al., 2000; Lohmann and Kärcher, 2002), which is often generated through cooling due to vertical air motion. Large scale updraughts cannot reproduce observed cirrus properties on their own, the smaller scale variation in updraught provided by gravity waves is necessary (Kärcher and Ström, 2003) and is occasionally able to produce cirrus in regions of large scale subsidence (Muhlbauer et al., 2014). These small scale updraughts can produce N_i values as high as 50,000 L^{-1} (Hoyle et al., 2005), highlighting the important role that vertical motion can play in determining the N_i.

Although ice can form by in-situ nucleation, many ice crystals also form through the freezing of liquid condensate. This liquid-origin cirrus often originates from high updraught regions in mixed-phase clouds, forming thicker cirrus that those composed of in-situ ice (Krämer et al., 2016; Luebke et al., 2016). Synoptic-scale updraughts can also produce liquid-origin cirrus in the mid-latitudes (Wernli et al., 2016). The N_i formed through these liquid-origin processes is also strongly dependent on the cloud-scale updraughts, with higher updraughts maintaining higher ice supersaturations and producing larger N_i values (Kärcher and Seifert, 2016; Kärcher, 2017).

Aerosol also plays a role in determining the N_i, although its impact is complicated by variations in ice crystal nucleation pathways and aerosol properties. While any particle can theoretically act as a homogeneous nucleation centre given a high enough supersaturation, in practice these aerosols are often hydrophilic liquid aerosols (Kojima et al., 2004). Increases in the aerosol number can result in an increase in N_i through increased homogeneous nucleation. However, in many situations, the N_i is limited by dynamical concerns, limiting the impact of aerosols (Lohmann and Kärcher, 2002; Kay and Wood, 2008).

Atmos. Chem. Phys. Discuss., https://doi.org/10.5194/acp-2018-21
Manuscript under review for journal Atmos. Chem. Phys.
Discussion started: 31 January 2018

Atmospheric Chemistry and Physics Discussions

A second class of aerosols, known as ice nucleating particles (INP) are able to nucleate ice heterogeneously and can freeze liquid water droplets at temperatures warmer than 235 K. At these warmer temperatures, the presence of INP will often control the N_i near nucleation locations (Kärcher and Lohmann, 2003), as they form the sites for creating an ice crystal, although the nucleating ability of these INP is also a strong function of temperature (Hoose and Möhler, 2012). As heterogeneous nucleation can take place at a lower supersaturation than homogeneous nucleation, the introduction of INP has the ability to prevent homogeneous nucleation by depressing the supersaturation. As the N_i produced through homogeneous nucleation events is typically higher than the INP concentration (and so the N_i from heterogeneous nucleation), this implies that the introduction of INP into a clean atmosphere can reduce the N_i (Kärcher and Lohmann, 2003). In-situ (Gayet et al., 2004) and satellite studies (Chylek et al., 2006) have provided some evidence for a possible decrease in N_i with increasing aerosol based on regional and hemispheric differences in ice crystal properties, although has proved difficult to conclusively link these N_i changes to a change in INP.

The relative role of heterogeneous and homogeneous nucleation in the atmosphere is unclear, making it difficult to develop observational constraints on the impact of aerosols on the N_i (e.g. Cziczo et al., 2013; Gasparini and Lohmann, 2016; Kärcher and Seifert, 2016). In addition, changing conditions over the lifecycle of a cloud can result in a switch between nucleation mechanisms (Krämer et al., 2016) and nucleation is not the only control on the N_i. The rarity of INP suggests that other processes, such as ice multiplication, are required to explain the N_i observed in the lower atmosphere (Heymsfield et al., 2017).

These four factors (temperature, supersaturation/updraught, ice origin and aerosol environment) are all thought to influence the N_i in high clouds, but there remain significant uncertainties in assessing the role of these factors on the N_i. First, the ice origin and in-cloud updraught are difficult to determine from observations at a large spatial and temporal scale. A recent classification (Gryspeerdt et al., 2017b) has shown some skill at determining these quantities when compared to a convection permitting model and is used in this work to account for this issue.

Second, the N_i is a difficult property to measure at a global scale. Aircraft measurements are limited in space and time and have been afflicted by shattering of crystals on the tips of measurement probes, casting doubt on some earlier measurements of the N_i (Korolev et al., 2013). Additionally, due to the highly variable nature of cirrus clouds and their strong sensitivity to environmental conditions, it can be difficult to separate the relative roles of aerosol and dynamics (Gayet et al., 2004).

The retrieval presented in part one of this work (Sourdeval et al., submitted) has demonstrated that the N_i can be retrieved using a combined radar-lidar retrieval and that this compares well to in-situ aircraft measurements. Combined with simultaneous retrievals of the ice water content, this allows the global distribution of the N_i and the factors that control it to be investigated. Using reanalysis aerosol concentrations and a proxy for the INP concentration, the impact of aerosols on high clouds is also investigated, highlighting avenues for future research into cirrus cloud processes.

Atmos. Chem. Phys. Discuss., https://doi.org/10.5194/acp-2018-21
Manuscript under review for journal Atmos. Chem. Phys.
Discussion started: 31 January 2018

Atmospheric Chemistry and Physics Discussions

2 Methods

The N_i dataset used in this work (DARDAR-LIM) has been described in detail in part one of this work (Sourdeval et al., submitted), so only the main features are outlined here. The DARDAR-LIM product is based on the DARDAR retrieval (Delanoë and Hogan, 2010), a combined raDAR-liDAR retrieval of ice cloud water content (IWC) and ice crystal effective radius using data from the CloudSat and CALIPSO satellites at approximately 13:30 local solar time. Only daytime data from the period 2006-2013 is used in this work due to constraints in the reanalysis data availability. The properties are retrieved at a horizontal resolution of 1.7 km and a vertical resolution of 60 m. Both the DARDAR IWC and the DARDAR-LIM N_i retrieval compare favourably to in-situ aircraft data (Deng et al., 2013; Sourdeval et al., submitted), with the best agreement at temperatures below -30°C, where the retrievals are more accurate due to the dominance of uni-modal ice crystal size distributions and reduced ambiguity in the cloud phase.

To investigate the controls on ice crystal nucleation, a more in-depth study is performed of the N_i near the cloud top ($N_{i(top)}$). As the cloud top is the location of the coldest temperature in the cloud, it provides a consistent location close to the nucleation sites within a cloud. This region is taken to be the top 120 m of the cloud and only the uppermost cloud layer (in multi-layer situations) is used to avoid issues with ice being seeded by ice crystals falling from overlying layers. The data is also restricted to locations where the retrieval has gone through at least two iterations, limiting the impact of prior assumptions about the cloud structure.

Four main controls on the $N_{i(top)}$ are considered in this work: temperature, cloud-scale updraught, ice origin and aerosol. Temperature data in this study is taken from the ECMWF ERA Interim reanalysis (Dee et al., 2011). Information about the cloud-scale updraughts and the ice-origin (liquid/ice) cannot yet be obtained directly at a global scale using satellites. To provide an indication of these cloud properties, the classification from Gryspeerdt et al. (2017b) is used. This classification is based on the assumed cirrus source (orographic, frontal, convective or synoptic) and determined at 13:30 local solar time using cloud retrievals from the MODIS instrument (Platnick et al., 2017) and reanalysis data. Through comparisons with convection permitting model data and classifications based on reanalysis data, this classification has been shown to provide useful information on the cloud scale updraughts and the ice origin. While not a direct retrieval these properties, it does allow some inferences to be made regarding the response of the N_i to these factors.

To investigate a possible aerosol link to N_i, we use the "monitoring atmospheric composition and climate" (MACC) aerosol re-analysis product (Morcrette et al., 2009; Benedetti et al., 2009), which assimilates MODIS aerosol optical depth (AOD) retrievals into the ECMWF integrated forecast system. The MACC product provides altitude information for aerosols along with speciation information. Although the MACC speciation has not yet been validated, the MODIS cloud droplet number concentration shows a stronger sensitivity to hydrophilic aerosol types that the hydrophobic ones, suggesting that the MACC speciation conveys useful information about the aerosol type (Gryspeerdt et al., 2016). Further from sources, where ageing and other assumptions come into play, the speciation may be less accurate. In the upper troposphere, liquid aerosol is thought to be the dominant aerosol component (Kojima et al., 2004). As such, this work takes the MACC total mass concentration as a measure of the liquid aerosol concentration, with high (low) aerosol being defined as being more (less) than 6 $\mu g\,m^{-3}$.

Atmos. Chem. Phys. Discuss., https://doi.org/10.5194/acp-2018-21
Manuscript under review for journal Atmos. Chem. Phys.
Discussion started: 31 January 2018

Atmospheric Chemistry and Physics Discussions

The response of the N_i to aerosol is likely to vary by aerosol type (Pruppacher and Klett, 1997). Although MACC provides a dust speciation, it is not clear whether this can be used to determine the presence of INP. Previous studies have suggested that high altitude aerosol may be responsible for glaciating clouds between 0°C and -35°C (Choi et al., 2010; Kanitz et al., 2011; Zhang et al., 2012; Tan et al., 2014). Based on this previous work, the glaciation of clouds between 0°C and -35°C is used as a proxy for the occurrence of INP.

Cloud phase is determined using the DARDAR phase detection algorithm (v1.1.4; Delanoë and Hogan, 2010). This uses the different response of lidar backscatter and radar reflectivity to liquid and ice hydrometeors to identify glaciated clouds. Clouds with a peak in lidar backscatter at the cloud top are treated as liquid or mixed phase and those with only a strong radar return are treated as glaciated. Experience suggests that the retrieved phase can be unreliable for clouds less than 600 m thick, so these are excluded from this part of the analysis.

Using this cloud top phase product, a "glaciation index" is developed for the mixed phase region. As approximately half of cloud tops are glaciated at -20°C, glaciated clouds with a top temperature warmer than -20°C are identified as "warm ice", and liquid topped clouds colder than -20°C are correspondingly "cold liquid". The "warm ice" pixels are taken to indicate the presence of INP within 100 km (the approximate spatial scale of aerosol variability from Weigum et al., 2012), whilst the "cold liquid" ones are taken to indicate a relatively INP-free environment. If both (or neither) are detected within 100 km, that pixel is excluded from the analysis. The cloud phase is only used for the uppermost cloud layer when determining this INP proxy to reduce the impact of overlying ice clouds seeding ice in lower layers. In addition, regions with nearby higher cloud layers (those within a 10:1 glide-slope) are also excluded from the "glaciation index". To reduce the impact of random errors in the phase retrieval, two or more neighbouring pixels are required for a detection of "warm ice" or "cold liquid".

This combination of reanalysis temperature and aerosol data, along with previously determined clouds regimes and a proxy for INP are used globally for daytime data over the period 2006-2013 to investigate the role of different processes on the N_i.

3 Results

3.1 Global $N_{i(top)}$ distribution

The global $N_{i(top)}$ distribution for crystals larger than 5μm ($N_{i(top)}^{5\mu m}$) displays several features that highlight the role of different cloud processes in controlling the $N_{i(top)}^{5\mu m}$. The zonal mean $N_{i(top)}^{5\mu m}$ (Fig. 1a) shows a strong temperature dependence, with significant increases in the $N_{i(top)}^{5\mu m}$ as the temperature decreases from a mean of around 40 L^{-1} at -35°C to almost 140 L^{-1} at -70°C. This temperature dependence is particularly strong at temperatures colder than -40°C in both the northern and the southern mid-latitudes. There is also a strong $N_{i(top)}^{5\mu m}$ increase in the tropics, although the initial increase in $N_{i(top)}^{5\mu m}$ at -40°C is weaker. This strong increase in $N_{i(top)}^{5\mu m}$ at -40°C along with a continuing N_i increase at colder temperatures is indicative of homogeneous nucleation, which is only significant at these lower temperatures.

At temperatures warmer than -35°C, the mean $N_{i(top)}^{5\mu m}$ is relatively small, especially in the northern hemisphere where it averages less than 50 L^{-1}. This is expected from heterogeneous nucleation, where the $N_{i(top)}^{5\mu m}$ is limited by available INP. The mean $N_{i(top)}^{5\mu m}$ is much larger in the southern hemisphere and the tropics, although this is skewed by the long tail of the

Atmos. Chem. Phys. Discuss., https://doi.org/10.5194/acp-2018-21
Manuscript under review for journal Atmos. Chem. Phys.
Discussion started: 31 January 2018

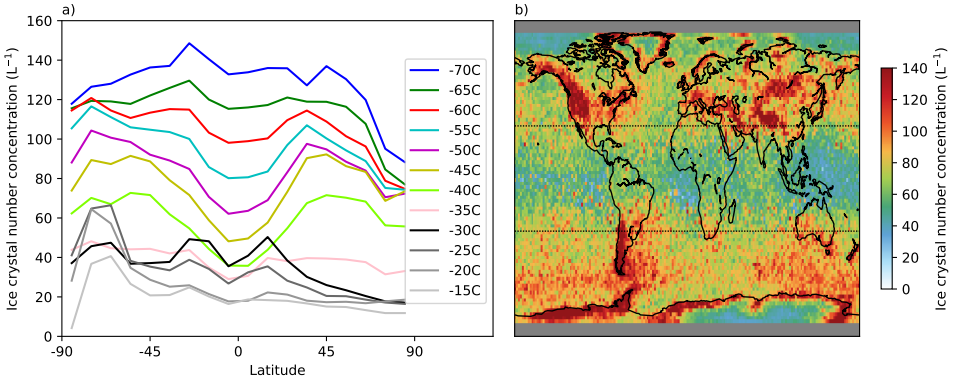

Figure 1. a) The zonal mean DARDAR-LIM cloud top N_i ($N_{i(top)}^{5\mu m}$) for crystals larger than 5 μm as a function of temperature from DARDAR-LIM data for the period 2006-2013. Temperatures warmer than -35°C are in greyscale. b) The mean $N_{i(top)}^{5\mu m}$ at -50°C. Grey indicates missing data.

$N_{i(top)}^{5\mu m}$ distribution (Fig. 2). A phase misclassification, with liquid topped cloud being mistaken for ice cloud might explain this hemispheric contrast. A strong lidar backscatter at the cloud top would lead to a large retrieved $N_{i(top)}^{5\mu m}$ (if it was mis-classified as an ice cloud). As liquid topped clouds at sub-zero temperatures are more common in the southern hemisphere, this would result in an erroneously large mean N_i in the southern hemisphere.

There are large geographical variations in $N_{i(top)}^{5\mu m}$. At -50°C, the $N_{i(top)}^{5\mu m}$ is strongly affected by the topography (Fig. 1b). High $N_{i(top)}^{5\mu m}$ values are retrieved in mountainous regions over land and around the edge of the Antarctic ice sheet, similar to results from orographic cirrus parametrisations in global climate models (e.g. Joos et al., 2008). This is consistent with a high $N_{i(top)}^{5\mu m}$ being generated through orographic uplift, which can generate the strong updraughts and high supersaturations required for homogeneous nucleation. While it is possible that the increased $N_{i(top)}^{5\mu m}$ is due to an increase in the vertical transport of INP, the lack of a similar pattern in the cloud supercooled fraction at -20°C (Choi et al., 2010) makes this explanation unsatisfactory. The $N_{i(top)}^{5\mu m}$ in the tropics is comparatively low, even in regions of significant topography such as the Ethiopian Highlands. This is due to low wind speeds in the tropics reducing the in-cloud orographic updraught, similar to the GCM results of Joos et al. (2008). The high orographic $N_{i(top)}^{5\mu m}$ also partially explains the hemispheric asymmetry in $N_{i(top)}$ in the mid-latitude and polar regions, due to the high $N_{i(top)}^{5\mu m}$ generated by orographic clouds over the Andes and around the edge of the East Antarctic ice sheet.

3.2 Cloud regime dependence

The location map and temperature dependence of the $N_{i(top)}^{5\mu m}$ (Fig. 1) and the results from part one hint that there may be a significant regime dependence in the $N_{i(top)}$, in particular a strong role for orographic clouds and a possible role for convective clouds, given the low $N_{i(top)}$ in the tropics. Separating the $N_{i(top)}$ data by regime using the classification of Gryspeerdt et al.

Atmos. Chem. Phys. Discuss., https://doi.org/10.5194/acp-2018-21
Manuscript under review for journal Atmos. Chem. Phys.
Discussion started: 31 January 2018

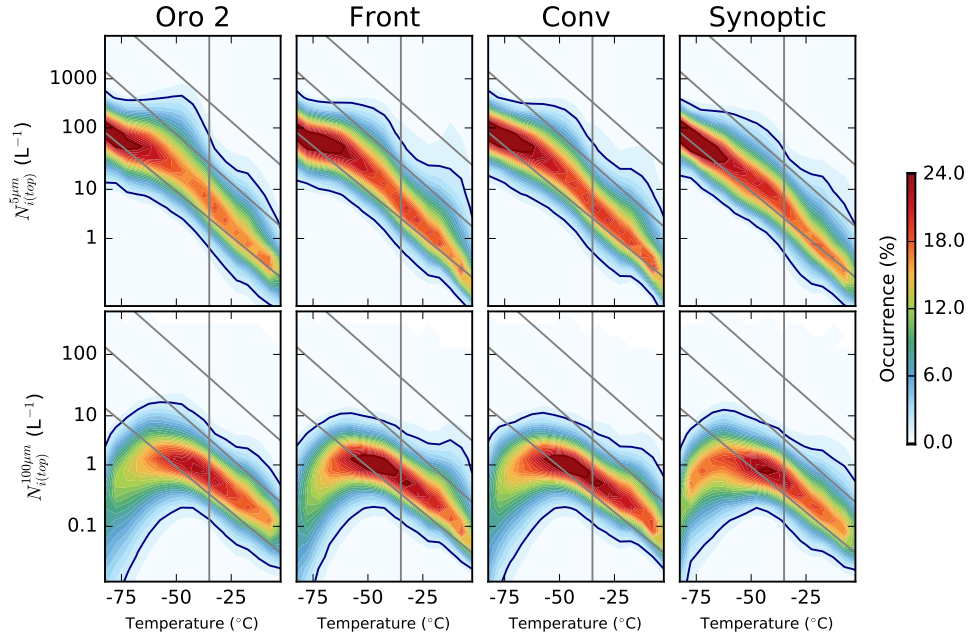

Figure 2. The conditional $N_{i(top)}$ (L^{-1}) for 5°C temperature bins for each of the main cloud regimes (Orographic, Frontal, Convective, Synoptic) from Gryspeerdt et al. (2017b, O2, F, C, S). The top row shows the $N_{i(top)}$ for particles greater than 5μm ($N_{i(top)}^{5\mu m}$) and the second greater than 100μm ($N_{i(top)}^{100\mu m}$). The columns are normalised so that they sum to 100%. Light grey lines are gridlines, the vertical line is drawn at -35°C - approximately the homogeneous nucleation threshold temperature and the diagonal lines are to aid comparison between the regimes. The regime names and definitions are given in Table 1 of Gryspeerdt et al. (2017a). Note the log scale for $N_{i(top)}$.

(2017b) allows this dependence to be independently investigated. Due to the strong temperature dependence and the large variability of the $N_{i(top)}$, joint probability histograms, showing the probability of a $N_{i(top)}$ retrieval at a given temperature are shown in Fig. 2. Following the results of part one, the $N_{i(top)}$ is investigated for crystals bigger than 5 μm ($N_{i(top)}^{5\mu m}$) and 100 μm ($N_{i(top)}^{100\mu m}$). With a minimum size of 5 μm, $N_{i(top)}^{5\mu m}$ typically lines up with the smallest sizes measured by in-situ instruments, while with a larger minimum size, $N_{i(top)}^{100\mu m}$ covers a size range where less shattering is expected and where the normalised size distribution performs well (Delanoë et al., 2005; Sourdeval et al., submitted).

There are a number of broad similarities between the regimes, each showing a clear increase in $N_{i(top)}^{5\mu m}$ with decreasing temperature, similar to results seen during the SPARTICUS campaign (Muhlbauer et al., 2014). The distribution becomes more sharply peaked in log space as the temperature reduces, rising to around 100 L^{-1} at -75°C. There is evidence of possible retrieval errors, as both the orographic and convective regimes have a small number of retrievals of over 30 L^{-1}, with some as high as 100 L^{-1}, around -15°C. This suggests that the possible phase misclassification and the high $N_{i(top)}$ values observed in the zonal mean are more common in certain regimes.

Atmos. Chem. Phys. Discuss., https://doi.org/10.5194/acp-2018-21
Manuscript under review for journal Atmos. Chem. Phys.
Discussion started: 31 January 2018

Atmospheric Chemistry and Physics Discussions

All of the regimes also show a peak in the $N_{i(top)}^{5\mu m}$ at temperatures just colder than -35°C. The strength varies by regime, with the orographic regime showing a strong peak and a weaker one being observed in the frontal and convective regimes. The peak is barely present in the synoptic regime. A strong increase in $N_{i(top)}^{5\mu m}$ at this temperature is consistent with homogeneous nucleation, either through an increase in the freezing of liquid droplets or through increased homogeneous nucleation directly into the ice phase.

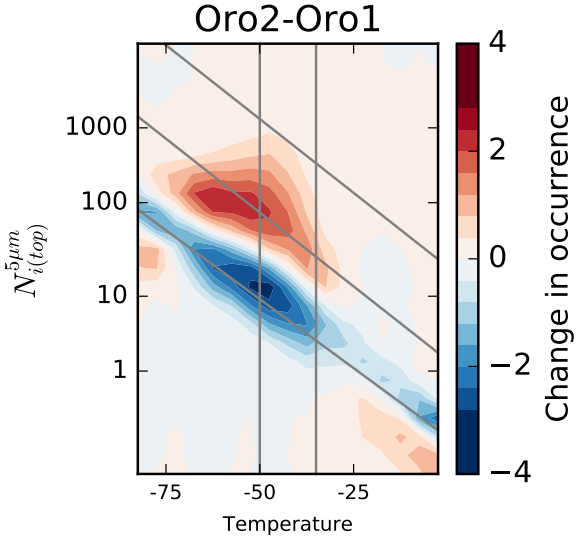

Figure 3. The difference the the $N_{i(top)}^{5\mu m}$ as a function of temperature between the Oro 2 and Oro 1 regimes (highest and second highest sextiles of estimated in-cloud updraught). Red above blue at a given temperature indicates an increased $N_{i(top)}^{5\mu m}$ in the Oro 2 regimes compared to Oro 1.

The variation in the strength of this peak is clearly seen when comparing the Oro 2 and Oro 1 regimes (the highest and second highest sextiles of the estimated in-cloud updraught) in Fig. 3. While there is little difference between the regimes at warmer temperatures, below -35 °C there is a strong increase in the $N_{i(top)}^{5\mu m}$ in the Oro 2 regime. This increase peaks at about -50 °C, reducing and almost disappearing at the coldest temperatures studied. The high $N_{i(top)}^{5\mu m}$ retrieved in these clouds and the strong dependence on the in-cloud updraught explain the geographical pattern shown in Fig. 1b, where high $N_{i(top)}^{5\mu m}$ are observed in mountainous regions. A high $N_{i(top)}^{5\mu m}$ in these regimes is supported by results from previous in-situ studies, where large N_i values were recorded in orographic clouds (Field et al., 2001).

It is possible that this increased $N_{i(top)}^{5\mu m}$ is the result of increased aerosol concentrations carried to lower temperatures in the stronger updraughts of the Oro 2 regime. However, the lack of a difference in $N_{i(top)}^{5\mu m}$ between the regimes at temperatures warmer than -35 °C indicates that an increase in INP is not driving this change in $N_{i(top)}^{5\mu m}$, which in turn makes it less likely that this change is due to a change in liquid aerosol. As the Oro regimes are defined by the estimated in-cloud updraught (Gryspeerdt et al., 2017b), the difference between the regimes shown in Fig. 3 is likely due to a change in the updraught environment.

Atmos. Chem. Phys. Discuss., https://doi.org/10.5194/acp-2018-21
Manuscript under review for journal Atmos. Chem. Phys.
Discussion started: 31 January 2018

Atmospheric Chemistry and Physics Discussions

A change in the updraught environment could modify the $N_{i(top)}^{5\mu m}$ by changing the likelihood of homogeneous nucleation, through an either increase in the number of activated CCN in the mixed-phase part of the cloud lifecycle or through allowing more liquid droplets to reach temperatures where they can freeze homogeneously. These processes cannot be easily distinguished in the current study, although the lack of a significant occurrence of liquid-topped cloud in orographic regions (Tan et al., 2014) suggests that an increased cloud droplet number concentration is not the leading contributor to the increase in $N_{i(top)}^{5\mu m}$. This strong response to updraught changes would support previous studies that highlighted the updraught limited nature of many cirrus clouds (Kay and Wood, 2008).

The temperature dependence of crystals larger than 100 μm ($N_{i(top)}^{100\mu m}$) at the cloud top displays a different pattern (Fig. 2, bottom row). While $N_{i(top)}^{100\mu m}$ and temperature are negatively correlated at warmer temperatures, the $N_{i(top)}^{100\mu m}$ reaches a peak at around -50 °C and there is a decrease in the $N_{i(top)}^{100\mu m}$ as temperatures reduce further, with the strongest decrease observed in the orographic regime. This is consistent with a shift towards smaller ice crystals at the cloud top with colder temperatures. The synoptic regime shows a weaker decrease in $N_{i(top)}^{100\mu m}$, indicating a slightly larger role for larger ice crystals in this regime. This shift towards smaller crystals at the cloud top is expected due to slower depositional growth and aggregation of ice crystals at colder temperatures resulting in crystals precipitating from the cloud top region before they grow larger than 100 μm.

3.3 The N_i within clouds

The behaviour of the N_i within clouds as a function of temperature displays some significant contrasts to the $N_{i(top)}^{5\mu m}$ (Fig. 4). While all of the regimes show an increase in the $N_i^{5\mu m}$ with decreasing temperature, this increase is much weaker than the increase in the $N_{i(top)}^{5\mu m}$. Similarly, although the peak that is visible in the $N_{i(top)}^{5\mu m}$ at about -40 °C is still visible in $N_i^{5\mu m}$ in the orographic and frontal regimes, it is much weaker than the peak observed at the cloud top. The synoptic regime has the strongest temperature dependence of all of the regimes. One explanation is the lower average cloud depth, such that the $N_i^{5\mu m}$ retrieved is often closer to the cloud top than in the other regimes. In all of the regimes, the $N_i^{5\mu m}$ is much larger in-cloud than at the cloud top for temperatures warmer than -30 °C, with values up to 100 L^{-1} being commonly observed. The smaller $N_i^{5\mu m}$ values that are more typically observed in the synoptic regime than the other regimes suggest that seasonal variations of the cloud classes (Gryspeerdt et al., 2017b) are likely responsible for the seasonal variations in $N_i^{5\mu m}$ observed in part one.

Similar to the $N_i^{5\mu m}$, the temperature dependence of the $N_i^{100\mu m}$ is very different internally within clouds compared to at cloud tops. The temperature dependence is much weaker, with almost no temperature dependence at temperatures warmer than -50 °C. There is a decrease in the $N_i^{100\mu m}$ at the lowest temperatures, similar to the decrease in the $N_{i(top)}^{100\mu m}$ seen in Fig. 2 and is explained by the retrievals at these temperatures being closer to the cloud top than at warmer temperatures. The synoptic regime has the lowest $N_i^{100\mu m}$ at warmer temperatures, which may again be due to the lower geometrical thickness of clouds in this regime, such that the $N_i^{100\mu m}$ is typically located closer to the cloud top, resulting in a lower $N_{i(top)}^{100\mu m}$ for any given temperature inside a cloud.

The larger $N_i^{100\mu m}$ values at warmer temperatures mean that larger crystals comprise a larger proportion of the $N_i^{5\mu m}$, with a reduced contribution of small crystals to the $N_i^{5\mu m}$. The weak temperature dependence of the $N_i^{100\mu m}$ is very similar to the aircraft results reported by Krämer et al. (2009), suggesting that the lack of a dependence on temperature in these previous

Atmos. Chem. Phys. Discuss., https://doi.org/10.5194/acp-2018-21
Manuscript under review for journal Atmos. Chem. Phys.
Discussion started: 31 January 2018

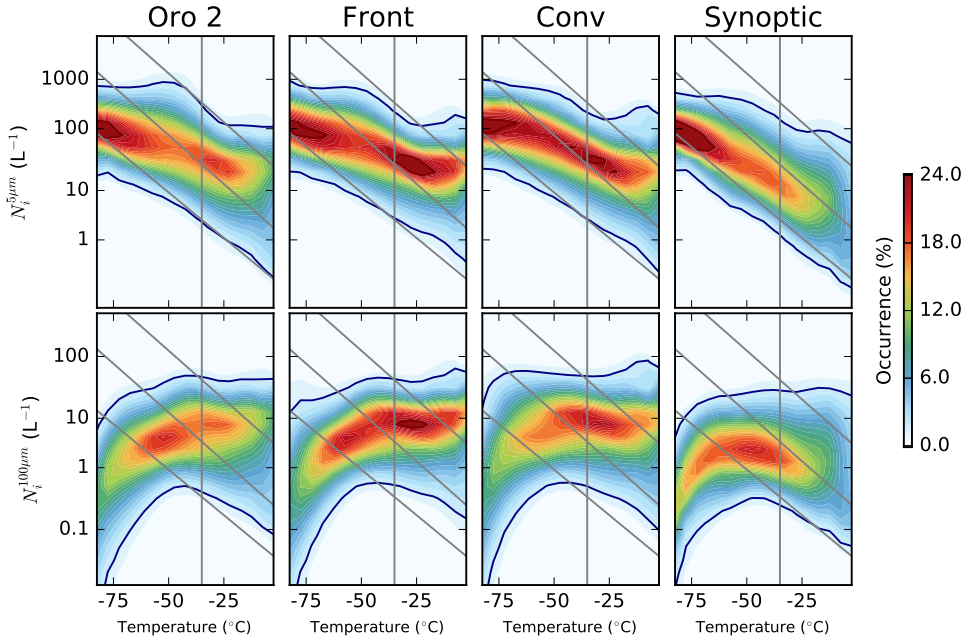

Figure 4. As Fig. 2 but using the N_i from throughout the cloud, rather than just the cloud top. The temperature scale is the temperature of the N_i retrieval, rather than that of the cloud top.

results could be due to a lack of measurements near the cloud top. It further suggests that as the N_i is strongly controlled by precipitating crystals from colder temperatures, the apparent mismatch between the INP and N_i concentration in aircraft data (e.g. Kanji et al., 2017) is due to the difficulty of sampling the nucleation region within a cloud. The retrieved $N_{i(top)}^{100\mu m}$ values at temperatures warmer than -35 °C (Fig. 2) are a much closer match to observed INP concentrations than the internal $N_i^{100\mu m}$.

3.4 Vertical structure of N_i

The $N_i^{5\mu m}$, $N_i^{100\mu m}$ and ice water content (IWC) all change significantly as a function of depth through the cloud (Fig. 5). For clouds with a top temperature between -50 and -60°C (Fig. 2), the $N_i^{5\mu m}$ continues to increase until about 500 m from the cloud top, at which point it starts to decrease again (Fig. 5, top row). The $N_i^{5\mu m}$ distribution width stays approximately constant from about 1 km into the cloud until around 2-3 km from the cloud top, when it reaches a temperature of around -30°C when liquid water can form more easily. At this point the $N_i^{5\mu m}$ distribution broadens significantly. Similar to the $N_i^{5\mu m}$, the $N_i^{100\mu m}$ also grows quickly when moving down through the cloud, moving to a slower growth regime after the first 500 m from the cloud top. This shift in the $N_i^{100\mu m}$ growth regime is roughly coincident with the location of the $N_i^{5\mu m}$ peak. All of the regimes also show an increase in the IWC (Fig. 5, bottom row) with increasing depth in the cloud, with a sharp increase over 2.5 km from

Atmos. Chem. Phys. Discuss., https://doi.org/10.5194/acp-2018-21
Manuscript under review for journal Atmos. Chem. Phys.
Discussion started: 31 January 2018

Atmospheric Chemistry and Physics Discussions

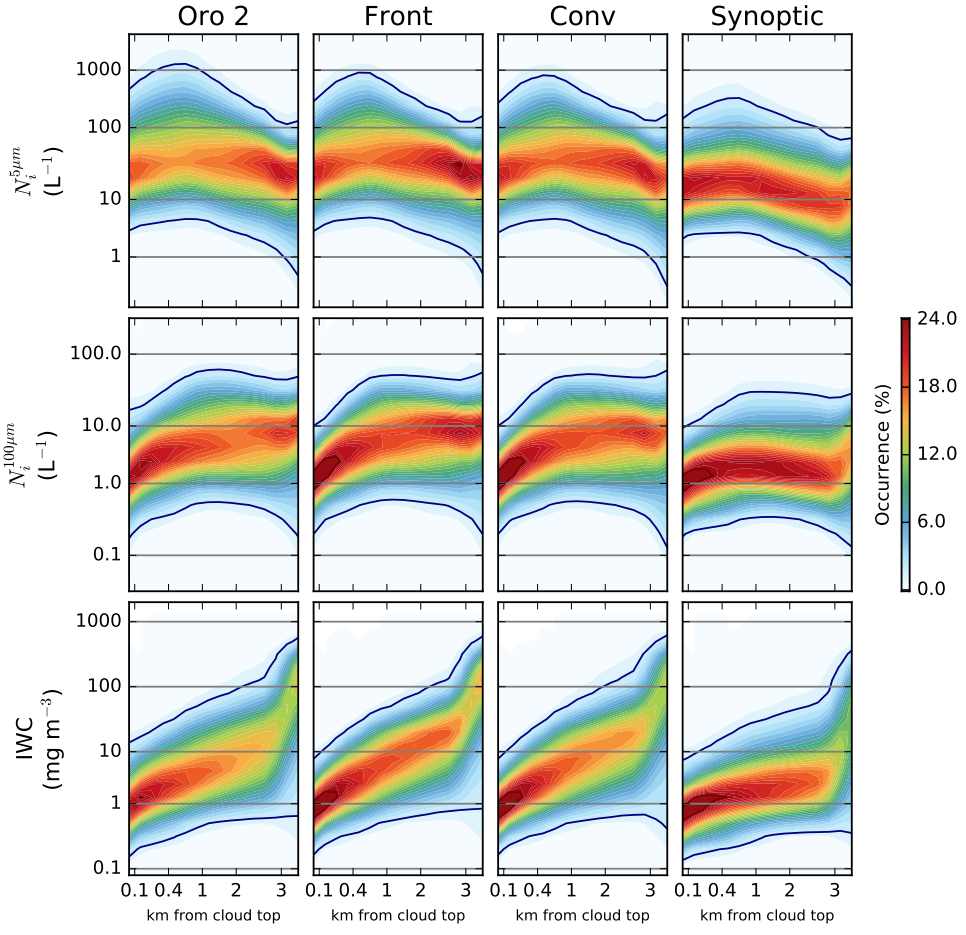

Figure 5. Retrieved properties as a function of the distance from the cloud top. This is for clouds with tops between -50 and -60 °C. Note the non-linear scale on the horizontal axis.

the cloud top. This sharp increase is consistent with a possible increase in ice through liquid water processes in warmer parts of the cloud.

There are some differences between the regimes. The synoptic regime has a much weaker peak in $N_i^{5\mu m}$ below the cloud top and a consequently lower $N_i^{5\mu m}$ throughout the depth of the regime. Despite having similar values at the cloud top to the other regimes, the $N_i^{100\mu m}$ and the IWC in the synoptic regime remain lower than the other regimes through the cloud. At about 2.5 km from the cloud top, both $N_i^{100\mu m}$ and IWC increase until they are roughly comparable to the other regimes, suggesting that the signal from liquid water swamps any signal based on ice nucleation.

It is possible that the $N_i^{5\mu m}$ peak is caused by the different sensitivities of the CloudSat radar and the CALIOP lidar, with the lower vertical resolution and sensitivity of the radar resulting in it missing the cloud top detected by the lidar. If this was

the case, the peak would likely be stronger and further from the cloud top in cases where the IWC is low (due to the increased penetration distance required for a significant radar return). However, the peak is weaker in the synoptic regime, where the IWC is lower than the other regimes, suggesting that the occurrence of this peak is not attributable to a retrieval error. The results from part one support this assessment, showing no clear signal of strong biases in the lidar-only to lidar-radar transition region.

The location of the peak may be related to the updraught in the cloud. As the crystal fall velocity is related to the crystal size, in a cloud with a fast enough updraught, the crystals have to grow to a significant size before they can fall through the cloud. If this is the case, the initial ice crystal nucleation region (and so the peak in $N_i^{5\mu m}$) would then exist further from the cloud top in clouds with a stronger updraught. This may explain the weaker $N_i^{5\mu m}$ peak in the synoptic regime, as this regime is expected to have weaker in-cloud updraughts (Gryspeerdt et al., 2017b). When the peak occurs in the synoptic regime, it is within 300 m of the cloud top in 67% of cases, compared to only 48% of cases for the frontal regime. The enhancement of the $N_i^{5\mu m}$ within this peak in the synoptic regime is also smaller, with an average peak of 130 L^{-1}, compared to 270 L^{-1} in the frontal regime and 325 L^{-1} for the orographic regime. This lends support to the hypothesis that the properties of this peak are related to the in-cloud updraught.

4 The impact of aerosol

4.1 The impact of liquid aerosol

Fig. 6 shows how the $N_{i(top)}^{5\mu m}$ distribution changes as a function of temperature and MACC reanalysis aerosol (used to indicate high concentrations of liquid aerosol). In most of the regimes, there is a positive relationship between MACC aerosol and $N_{i(top)}^{5\mu m}$ at temperatures below -35 °C (shown by red above blue in Fig. 6). In the synoptic regime, this positive aerosol-$N_{i(top)}^{5\mu m}$ relationship only exists for temperatures warmer than -60 °C – at temperatures colder than this, the relationship becomes weak and noisy. In the other regimes, the positive relationship is maintained to very cold temperatures. At temperatures warmer than -35 °C, the relationship becomes a lot weaker, with almost no aerosol-$N_{i(top)}^{5\mu m}$ relationship existing in the orographic and convective regimes. In the frontal regime, there is a slight negative relationship, with a stronger negative relationship in the synoptic regime. It is possible that this negative relationship is related to a misclassification of ice and liquid at these warmer temperatures being a function of the MACC aerosol.

The aerosol-$N_{i(top)}^{100\mu m}$ relationship shows a weaker pattern than the aerosol-$N_{i(top)}^{5\mu m}$ relationship, with the smaller enhancement of the $N_{i(top)}^{100\mu m}$ at colder temperatures in most regimes indicating a shift to smaller crystal sizes. The change in the synoptic regimes is the strongest, likely related to the strong relationship for the $N_{i(top)}^{5\mu m}$.

A strong relationship between MACC aerosol and $N_{i(top)}$ could be due to increased ice crystal nucleation through homogeneous nucleation, which can be sensitive to the concentration of liquid aerosol (e.g. Kärcher and Seifert, 2016). In situations where the $N_{i(top)}$ is primarily determined by the freezing of liquid droplets, an increase in cloud droplets in high aerosol regions could also lead to an increased $N_{i(top)}$. As with the impact of in-cloud updraught on $N_{i(top)}$, further investigation is required to determine if one of these mechanisms is dominant. As liquid water has been found in clouds at temperatures as cold as -40°C,

Atmos. Chem. Phys. Discuss., https://doi.org/10.5194/acp-2018-21
Manuscript under review for journal Atmos. Chem. Phys.
Discussion started: 31 January 2018

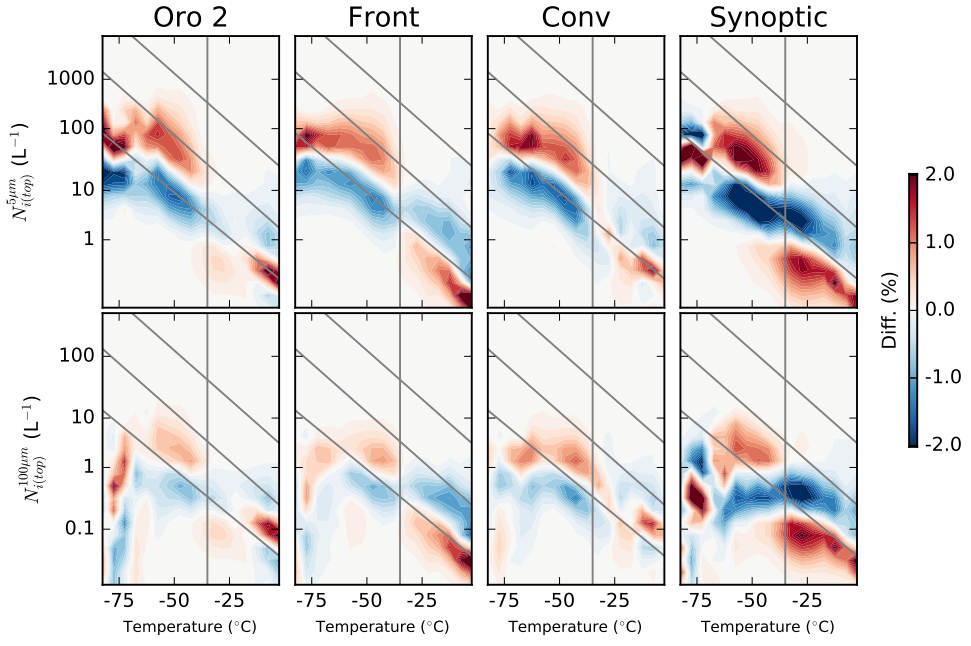

Figure 6. The difference in the conditional histograms between cases with high MACC total aerosol mass concentration ($>6\mu g\,m^{-1}$) and low total mass concentration ($<6\mu g\,m^{-1}$) for the four main regimes. The gridlines are the same as Fig. 2. The upper set of plots show the difference in $N_{i(top)}^{5\mu m}$ and the lower in $N_{i(top)}^{100\mu m}$. The changes sum to zero vertically, red over blue indicates an increase in the $N_{i(top)}^{5\mu m}/N_{i(top)}^{100\mu m}$ for a given temperature and regime.

increased droplet freezing cannot be ruled out, even though many clouds are frozen before reaching this temperature (Choi et al., 2010). At colder temperatures, it seems likely that homogeneous nucleation plays a role, as liquid droplets cannot form at these temperatures. In this case, the stronger updraughts in the frontal and convective regimes are important for generating the high supersaturations in which homogeneous nucleation can occur. This would also explain the weak relationship between the N_i and MACC aerosol at colder temperatures in the synoptic regime, as the updraughts in this regime are weaker and so less likely to achieve the necessary supersaturations (Krämer et al., 2016).

4.2 The impact of INP

The sparse nature of INP measurements (e.g. Mamouri and Ansmann, 2016) and the high sensitivity of the N_i to low INP concentrations means that it is difficult to use retrieved aerosol properties to investigate the effect of INP on the $N_{i(top)}$. To avoid this issue, the glaciated fraction of clouds lower in the atmosphere (-20°C) is used as a proxy for the presence of INP at other levels in the atmosphere.

Atmos. Chem. Phys. Discuss., https://doi.org/10.5194/acp-2018-21
Manuscript under review for journal Atmos. Chem. Phys.
Discussion started: 31 January 2018

Atmospheric Chemistry and Physics Discussions

4.2.1 Cloud glaciation and INP

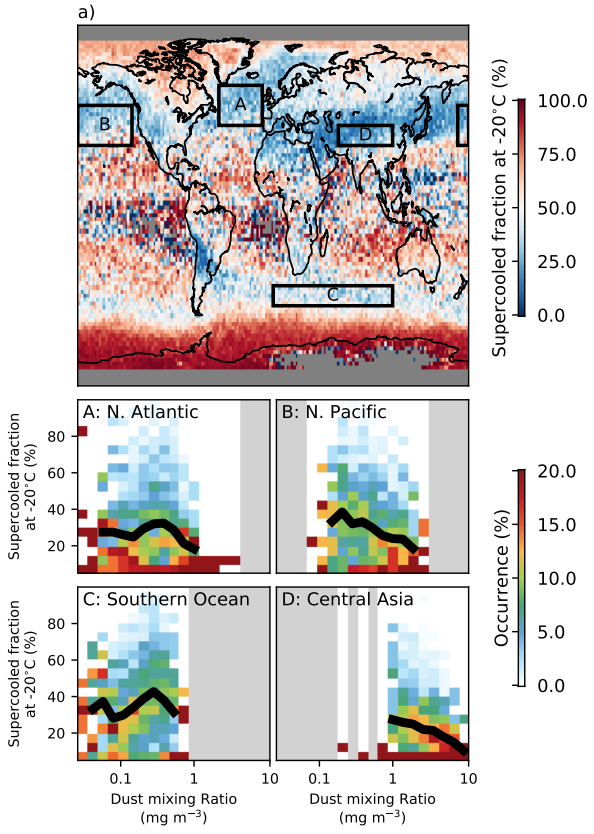

Figure 7. a) The DARDAR supercooled fraction at -20°C, defined as the fraction of DARDAR cloud top phase retrievals between -17.5 and -22.5 °C from 2006 and 2013 that are classed as liquid. b) The conditional probability of observing a daily mean supercooled fraction, given a specified MACC dust mixing ratio for the regions specified in (a). The black line shows the mean supercooled fraction for each aerosol bin.

The addition of the CloudSat data in the DARDAR product allows smaller quantities of ice to be detected than the lidar-only studies, but produces a very similar pattern of cloud glaciation (Fig. 7) to the previous CALIOP studies (Choi et al., 2010; Tan et al., 2014). Calculating the supercooled fraction as the number of liquid retrievals divided by the total number of liquid and ice retrievals between -17.5 °C and -22.5 °C from 2006 and 2013, using only the top layer of clouds where the layer is more than 600 m thick.

There is a strong hemispheric contrast with a higher glaciated fraction over the northern hemisphere and a high supercooled fraction over the southern ocean and Antarctica, as observed in previous aircraft (Huang et al., 2012) and satellite studies (Choi et al., 2010; Tan et al., 2014). High glaciated fractions are observed over desert locations in central Asia and Iran, stretching across the North Pacific to the Americas. This is consistent with previous studies suggesting that dust is a good INP. Previous

studies have found Asian dust over California, suggesting that transport across the Pacific is not unexpected (Creamean et al., 2013). There is also a significant proportion of glaciated cloud downwind of the Andes, which appears to originate near the Altiplano and Patagonia. These are sources of high altitude dust (Ginoux et al., 2012) and would support the hypothesis that high altitude dust is able to glaciate clouds. While glaciated cloud in this region has been previously noted (Choi et al., 2010), the lower resolution of the previous study made it difficult to determine the source of possible INP. The longer dataset and increased spatial resolution of Fig. 7a make the source in the upper Andes much clearer. Although southern Africa and Australia are also sources of dust (Ginoux et al., 2012), this dust is emitted at lower altitudes, which would explain the lower glaciated fractions downwind of these regions.

The origin of the glaciated region over the north Atlantic is less clear, as there are not many local sources of high level dust in the region. It is possible that the dust here has been transported across the Sahara and lofted by cyclone systems crossing the Atlantic. It is also possible the black carbon or ash (Grawe et al., 2016) from North America may act as an INP. This might explain the higher supercooled fraction over Siberia, where black carbon from fires typically occurs without the other aerosols that are found in industrial pollution, allowing it to act as an INP (Rosenfeld et al., 2011).

The ice nucleating impact of dust for driving the cloud glaciated fraction is supported by comparing the cloud glaciated fraction to reanalysis aerosol fields(Fig. 7b). There is a strong negative correlation between the occurrence of supercooled liquid cloud at -20°C and the mass concentration of reanalysis dust (Fig. 7b), with glaciated cloud dominating at high mass concentrations of reanalysis dust. However, this correlation varies by region. A stronger relationship is found in regions close to dust sources, such as over the N. Pacific (B) and central Asia (D). The relationship is much weaker in the N. Atlantic (A) and the southern ocean (C) where the dust is further from source.

The stronger dust-glaciation relationship close to the dust source, where the MACC aerosol speciation is best suggests that the supercooled fraction of clouds at -20°C is strongly related to the occurrence of INP. The weaker relationship further from source suggests that although the MACC speciation has been shown to provide useful information on aerosol type, this speciation is less reliable further from source. This is supported by results in liquid clouds, where the dust optical depth-cloud droplet number concentration relationship becomes stronger further from dust sources (Gryspeerdt et al., 2016).

Due to the reduced speciation skill from MACC far from dust sources, the occurrence of glaciated cloud at -20°C is used as a proxy for the occurrence of INP instead of the reanalysis aerosol. This relies on two assumptions:

1. Cloud glaciation at -20°C is related to INP at -20°C
2. INP at -20°C is correlated to INP at other temperatures

Based on the relationship to MACC dust aerosol, the first assumption holds in many cases. Although the second assumption is tenuous, there is very unlikely to be a negative correlation between the INP at the two temperature levels, with the worst case being no correlation. As such, the relationship between the N_i and the INP proxy is unable to give a quantitative result for the impact of INP on the $N_{i(top)}^{5\mu m}$, but it is able to provide a qualitative indication of the sign of the INP impact.

Atmos. Chem. Phys. Discuss., https://doi.org/10.5194/acp-2018-21
Manuscript under review for journal Atmos. Chem. Phys.
Discussion started: 31 January 2018

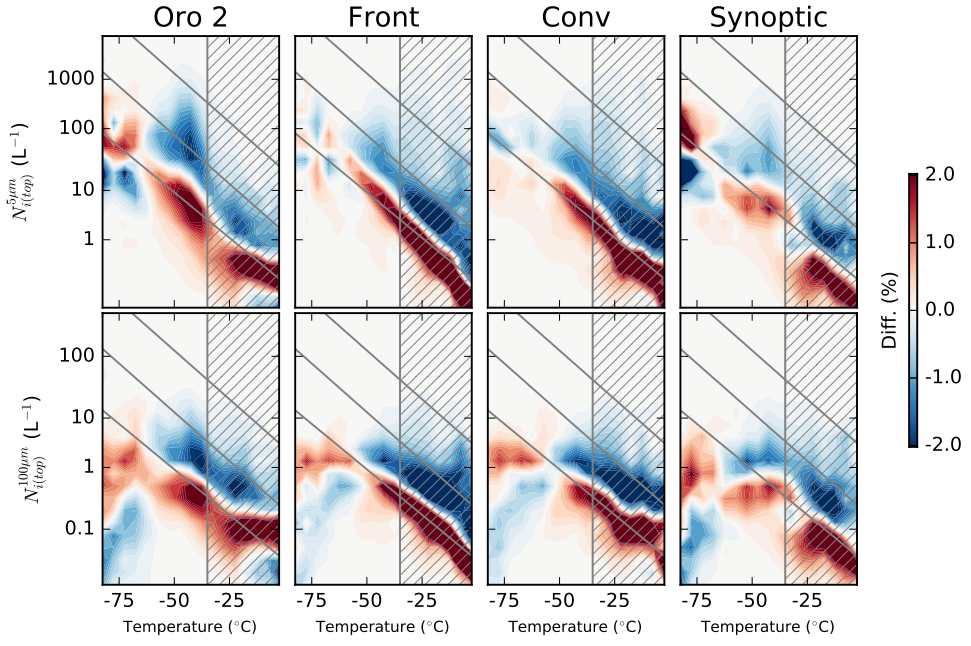

Figure 8. As Fig. 6 but showing the difference in the conditional histograms as a function of the INP proxy. Red indicates an increase in occurrence of a particular bin at higher inferred INP and blue a decrease, such that red above blue indicates an increase in $N_{i(top)}$ with increased INP for a given temperature. The shaded regions are likely affected by a phase misclassification at warmer temperatures.

4.2.2 The INP relationship to $N_{i(top)}$

The relationship of the $N_{i(top)}^{5\mu m}$ to the proxy for INP is shown in Fig. 8. There are a number of features that are similar between the regimes, in particular the strong negative relationship between INP occurrence and $N_{i(top)}^{5\mu m}$ at temperatures warmer than -35 °C. As with the large mean $N_{i(top)}^{5\mu m}$ values shown in Fig. 1a, this may be due to liquid clouds being misclassified as ice, resulting in large $N_{i(top)}^{5\mu m}$ values being retrieved. The requirement for "warm-ice" means that supercooled liquid occurs less frequently in the high INP cases, and as such it is less likely to be misclassified as ice. The lower frequency of this misclassification then reduces the $N_{i(top)}^{5\mu m}$ and $N_{i(top)}^{100\mu m}$ in cases of high INP. The weaker $N_{i(top)}^{5\mu m}$ response in the synoptic and orographic regimes supports this, as the misclassification in these regimes is weaker (Fig. 2). The warmer temperatures are shaded out in Fig. 8 due to the impact of this potential misclassification.

At colder temperatures, the INP-$N_{i(top)}^{5\mu m}$ relationship starts to vary between the regimes. All of the regimes show a decrease in the $N_{i(top)}^{5\mu m}$ between around -35 °C and -50 °C, the temperatures where the strong peak in $N_{i(top)}^{5\mu m}$ is observed connected with in-cloud updraught (Fig. 3). This decrease is strongest in the orographic regime and weakest in the synoptic regime, similar to the $N_{i(top)}^{5\mu m}$ peak observed observed in the different regimes (Fig. 2), lending support to the idea that this reduction in $N_{i(top)}^{5\mu m}$ is due to a suppression of homogeneous nucleation by INP.

Atmos. Chem. Phys. Discuss., https://doi.org/10.5194/acp-2018-21
Manuscript under review for journal Atmos. Chem. Phys.
Discussion started: 31 January 2018

Atmospheric Chemistry and Physics Discussions

At temperatures colder than -50 °C, the relationship becomes different again. In all of the regimes, there is an increase in $N_{i(top)}^{100\mu m}$ with increasing INP. This is consistent with an increasing number of INP shifting the size distribution towards larger ice crystals. In the orographic and synoptic regimes, this increase also appears in the $N_{i(top)}^{5\mu m}$, suggesting that in these cases, increasing the INP can increase even the numbers of small ice crystals. This might suggest that at the coldest temperatures, INP have a controlling influence on the $N_{i(top)}^{5\mu m}$ in these regimes, as would be the case if heterogeneous nucleation was dominant in these clouds. This would fit with the results from Fig. 6, where at the coldest temperatures, there was a relatively small response of the $N_{i(top)}^{5\mu m}$ to MACC total (liquid) aerosol, suggesting that homogeneous nucleation was not controlling the $N_{i(top)}^{5\mu m}$ in synoptic cirrus. At these coldest temperatures, dust can act as an INP at very low supersaturations (as low as 105%; Möhler et al., 2006), which may explain the dominance of heterogeneous nucleation at these temperatures.

5 Vertical information propagation

The changes in $N_{i(top)}^{5\mu m}$ observed in the previous section have impacts throughout the depth of the cloud. Fig. 9 shows how N_i and IWC information propagates vertically within a cloud. The cloud profiles are split into two categories, based on whether they have above or below median values of the cloud top properties ($N_{i(top)}$, $IWC_{(top)}$). The difference in the vertical structure of the clouds (in a similar manner to Fig. 5) is shown, with red over blue indicating that an increase in the retrieved quantity at a given distance from the cloud top for profiles that were above median in that property at the cloud top.

The top row of Fig. 9 shows that $N_i^{5\mu m}$ information propagates a significant distance through the cloud. Clouds with an increased $N_{i(top)}^{5\mu m}$ maintain a higher $N_i^{5\mu m}$ at distances at least 3km from the cloud top in all regimes. However, as shown in the second row, vertical information about the $N_i^{100\mu m}$ does not propagate nearly as far through the cloud. The vertical propagation is the highest in the synoptic regime. The vertical propagation of IWC information is very similar to the $N_i^{100\mu m}$, with the relationship to the cloud top IWC being significantly reduced more than 500 m from the cloud top.

The large vertical propagation of the $N_i^{5\mu m}$ indicates that the changes in $N_i^{5\mu m}$ at the cloud top found in the previous section can have considerable impact at lower levels in the cloud. However, the lower vertical propagation of the information about the larger crystals ($N_i^{100\mu m}$, IWC) would support the suggestion that the growth of the ice crystals after nucleation is primarily controlled by meteorological factors that do not play a large role in the nucleation processes that control $N_i^{100\mu m}$. Note that the temperature of the cloud top and the distance from the cloud top can still play a large role in determining the N_i (Figs. 4, 5).

6 Discussion

These results show that the $N_{i(top)}^{5\mu m}$ is strongly affected by several factors including temperature (Fig. 1), cloud type (Fig. 2) and updraught (Fig. 3) and that changes in the $N_{i(top)}^{5\mu m}$ can be maintained at large distances from the cloud top (Fig. 9). The dependence of the $N_{i(top)}^{5\mu m}$ on the in-cloud updraught and the relationship to reanalysis liquid aerosol (Fig. 6) suggests that at temperatures between -35 °C and -50 °C, the $N_{i(top)}^{5\mu m}$ is strongly affected by homogeneous nucleation processes. This is supported by the relationship of the $N_{i(top)}^{5\mu m}$ to the INP proxy (Fig. 8), where a reduction in $N_{i(top)}^{5\mu m}$ with increasing INP could

Atmos. Chem. Phys. Discuss., https://doi.org/10.5194/acp-2018-21
Manuscript under review for journal Atmos. Chem. Phys.
Discussion started: 31 January 2018

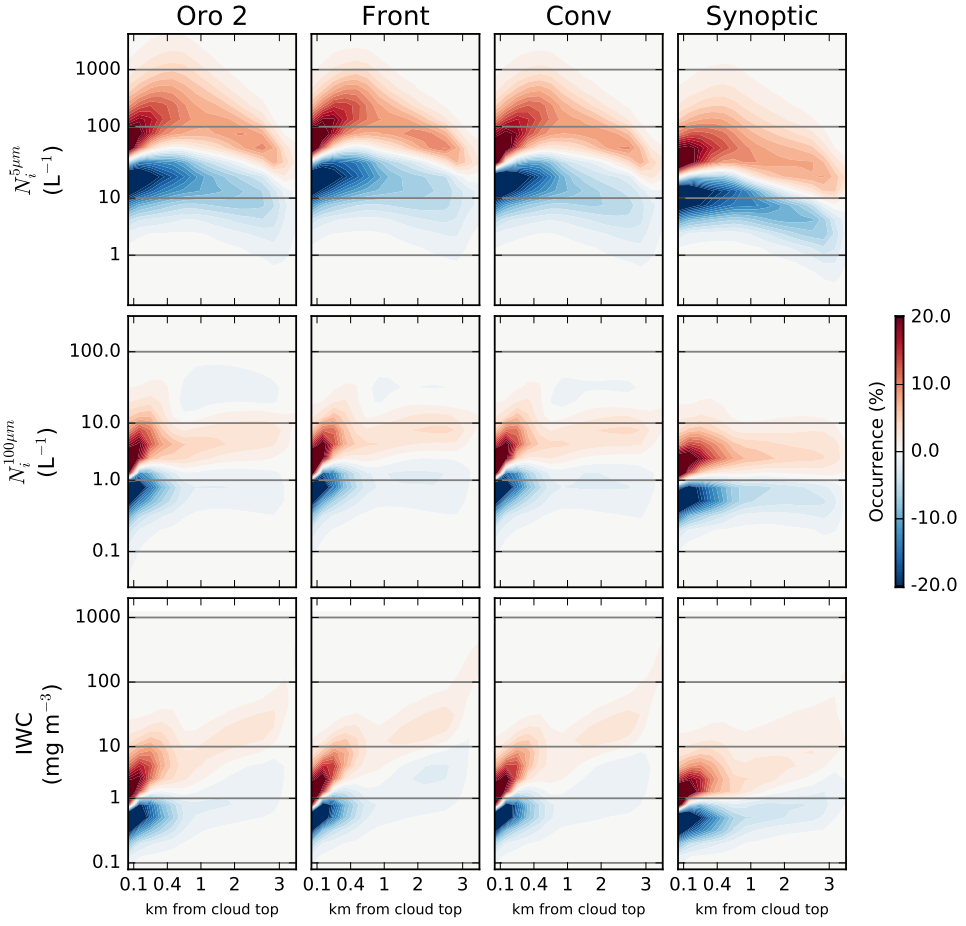

Figure 9. As Fig. 5, but showing the difference in the retrieved properties depending on the cloud top properties. Red over blue indicates that clouds with above median properties at the cloud top ($N_{i(top)}^{5\mu m}$, $IWC_{(top)}$) have higher values of the retrieved properties at a specified depth from the cloud top. Note the non-linear scale on the horizontal axis.

be indicative of a negative Twomey effect. The relationship with INP also suggests that at temperatures colder than -50 °C, heterogeneous nucleation has a strong role to play in determining the $N_{i(top)}^{5\mu m}$ in synoptic cirrus clouds.

Uncertainties in the retrieval have been covered in part one of this work (Sourdeval et al., submitted). However, there are a few points to note with regards to the relationship of the N_i to other cloud and meteorological properties. Although there is significant uncertainty in the N_i retrieval, many of these uncertainties are random errors and not systematic functions of the meteorological properties investigated here. Even ice crystal shape, which can be a major issue in ice cloud retrievals, is a function of temperature (to first order) and so does not impact the majority of the results which are presented in this work stratified by temperature.

Atmos. Chem. Phys. Discuss., https://doi.org/10.5194/acp-2018-21
Manuscript under review for journal Atmos. Chem. Phys.
Discussion started: 31 January 2018

Atmospheric Chemistry and Physics Discussions

The cloud phase classification is of critical importance to the warmer clouds included in this study and there is evidence of a misclassification of a small number of cases (Fig. 8) at temperatures warmer than -35 °C. This can make it difficult to interpret results at these temperatures, so they are not a focus of this work. The change in phase of these clouds as a function of aerosol is likely to dominate the radiative response of clouds to aerosols at these temperatures.

There are a number of limitations of this study that could be addressed in future work. The lack of information about the location of INP is a serious issue when investigating the impact of aerosol on N_i. While the INP proxy in this work is able to provide a qualitative estimate of the role of INP in determining the N_i, for a quantitative estimate a better proxy or measure of the global INP concentration is required.

Additionally, the lack of observations of in-cloud updraughts also limits how accurately the impact of aerosol on the N_i can be determined. Although the cloud regimes used have some ability to constrain the cloud-scale updraught (Gryspeerdt et al., 2017b), the updraught is a critical component in determining the N_i through it's influence on the supersaturation. The in-cloud updraught is assumed to be largely independent of the aerosol properties in this work, but it is possible that the reanalysis aerosol is related to the in-cloud updraught, such that more aerosol is transported vertically in conditions with high in-cloud updraughts. In this case, a positive correlation between the N_i and MACC reanalysis aerosol could be generated. However, as MACC does not explicitly simulate in-cloud updraughts, the impact of this confounding issue is likely to be small.

It is also possible that using cloud glaciation as a proxy allows other meteorological covariations, which could generate apparent relationships between the "INP" and N_i. However, the in-cloud updraught is of a second order importance in determining the cloud-top phase compared to the INP concentration (Bühl et al., 2013). The inclusion of a "glide-slope" test when determining the INP proxy means that it is also unlikely that clouds are being glaciated but undetected ice falling from higher cloud layers. The separation into cloud regimes also limits the impact of these kind of meteorological covariations, which might be expected between different regimes, but would be weaker within them.

The behaviour of the N_i retrieval in this work follows the expected behaviour of the N_i determined in several previous studies based on in-situ, theoretical and modelling results. This provides further evidence that the DARDAR-LIM N_i retrieval described in (Sourdeval et al., submitted) is able to retrieve the N_i in a variety of situations.

7 Conclusions

Few global studies exist of the controls on the ice crystal number concentration (N_i), especially the role of aerosols. In this study, the DARDAR-LIM N_i retrieval from part one (Sourdeval et al., submitted) is used to investigate possible controls on the N_i at a global scale. A special emphasis is placed on the N_i at the cloud top ($N_{i(top)}$), due to it's close proximity to ice crystal nucleation locations within high clouds.

Strong impacts on the $N_{i(top)}$ are observed for updraught, cloud type and particularly temperature (Figs. 1, 2), with a higher $N_{i(top)}$ for crystals larger then 5μm ($N_{i(top)}^{5\mu m}$) being found at colder temperatures in all regimes, consistent with an increased nucleation rate at lower temperatures. Fewer crystals larger than 100μm, ($N_{i(top)}^{100\mu m}$) are found at the coldest temperatures,

possibly due to the reduced depositional growth rate removing them from the cloud top region before they can grow to a sufficient size.

Many of the regimes show an increase in the $N_i^{100\mu m}$ and a decrease in the $N_i^{5\mu m}$ with increasing distance from the cloud top (Fig. 5) due to the aggregation of ice crystals as they sediment within the cloud. The rate of change of the N_i moving away from the cloud top depends on the regime, with much slower changes in the synoptic regime indicating a role of meteorological factors in determining ice crystal growth rates. This is supported by the weaker temperature dependence of the N_i within clouds compared to the $N_{i(top)}$ (Fig. 4), which may also explain the apparent weak dependence of N_i on temperature (Krämer et al., 2009) and INP (Kanji et al., 2017) found in previous studies. Given the large difference between the $N_{i(top)}$ and the N_i deeper in the cloud, this may suggest that the cloud top would make a good target for future in-situ campaigns examining the controls on ice nucleation.

There are indications of homogeneous nucleation or the freezing of liquid droplets determining the $N_{i(top)}$. A temperatures just colder than -35°C, there is a strong peak in the $N_{i(top)}^{5\mu m}$ (Fig. 2). This peak is related to the updraught strength in the cloud, with the reliably high updraughts in the orographic regime giving it the strongest peak (Fig. 3). This is further supported by the relationship between the $N_{i(top)}^{5\mu m}$ and the MACC reanalysis aerosol (Fig. 6), with an increased $N_{i(top)}^{5\mu m}$ being observed in high aerosol environments, indicating a possible dependence on the liquid aerosol concentration, particularly for smaller crystals.

As previous work has suggested that INP occurrence is related to cloud glaciation, the glaciated fraction at -20° is used as a qualitative proxy for INP occurrence (Fig. 7). At temperatures between -50°C and -35°C, there is a reduction in $N_{i(top)}^{5\mu m}$ with increasing "INP" (Fig. 8), which may indicate a "negative Twomey" effect in action (Kärcher and Lohmann, 2003) and provide further supporting evidence for the role of homogeneous nucleation in determining the $N_{i(top)}$. At colder temperatures, some regimes show an increasing $N_{i(top)}$, and the $N_{i(top)}^{100\mu m}$ in particular, which may be evidence of heterogeneous nucleation controlling the $N_{i(top)}$ and shifting the size distribution towards larger crystals. Further studies are required to separate the role of these different mechanisms in controlling the $N_{i(top)}$.

While changes to the $N_{i(top)}$ are important for radiative considerations, changes in the $N_{i(top)}$ can have implications for the cloud many kilometres below the cloud top (Fig. 9). This far reaching impact into the lifecycle of ice and mixed-phase clouds demonstrates the importance of developing strong observational constraints on the controlling factors of the N_i. The results presented in this work provide a global context for existing theory and in-situ measurement based hypotheses about cloud properties, highlighting areas for future research to further constrain ice and mixed-phase cloud processes.

Acknowledgements. The MODIS data are from the NASA Goddard Space Flight Center (ftp://laadsweb.nascom.nasa.gov). The DARDAR data product were retrieved from the ICARE data center (http://www.icare.univ-lille1.fr). The MACC reanalysis data is available on-line at (http://apps.ecmwf.int/datasets/data/macc-reanalysis). This work was supported by funding from the European Research Council under the European Union's Seventh Framework Programme (FP7/2007-2013) / ERC grant agreement no. FP7-306284 ("QUAERERE"); the Bundesministerium für Bildung und Forschung, grant numbers 01LK1210D, 01LK1503A and 01LK1505E; and Deutsche Forschungsgemeinschaft, grant number QU 311/14-1. EG is supported by an Imperial College Junior Research Fellowship.

References

Benedetti, A., Morcrette, J.-J., Boucher, O., Dethof, A., Engelen, R. J., Fisher, M., Flentje, H., Huneeus, N., Jones, L., Kaiser, J. W., Kinne, S., Mangold, A., Razinger, M., Simmons, A. J., and Suttie, M.: Aerosol analysis and forecast in the European Centre for Medium-Range Weather Forecasts Integrated Forecast System: 2. Data assimilation, J. Geophys. Res., 114, D13 205, https://doi.org/10.1029/2008JD011115, 2009.

Boucher, O., Randall, D., Artaxo, P., Bretherton, C., Feingold, G., Forster, P., Kerminen, V.-M., Kondo, Y., Liao, H., Lohmann, U., Rasch, P., Satheesh, S., Sherwood, S., Stevens, B., and Zhang, X.: Clouds and Aerosols, book section 7, p. 571–658, Cambridge University Press, Cambridge, United Kingdom and New York, NY, USA, https://doi.org/10.1017/CBO9781107415324.016, www.climatechange2013.org, 2013.

Bühl, J., Ansmann, A., Seifert, P., Baars, H., and Engelmann, R.: Toward a quantitative characterization of heterogeneous ice formation with lidar/radar: Comparison of CALIPSO/CloudSat with ground-based observations, Geophys. Res. Lett., 40, 4404–4408, https://doi.org/10.1002/grl.50792, 2013.

Choi, Y.-S., Lindzen, R. S., Ho, C.-H., and Kim, J.: Space observations of cold-cloud phase change, Proc. Natl. Acad. Sci., 107, 11 211–11 216, https://doi.org/10.1073/pnas.1006241107, 2010.

Chylek, P., Dubey, M. K., Lohmann, U., Ramanathan, V., Kaufman, Y. J., Lesins, G., Hudson, J., Altmann, G., and Olsen, S.: Aerosol indirect effect over the Indian Ocean, Geophys. Res. Lett., 33, L06 806, https://doi.org/10.1029/2005GL025397, 2006.

Creamean, J. M., Suski, K. J., Rosenfeld, D., Cazorla, A., DeMott, P. J., Sullivan, R. C., White, A. B., Ralph, F. M., Minnis, P., Comstock, J. M., Tomlinson, J. M., and Prather, K. A.: Dust and biological aerosols from the Sahara and Asia influence precipitation in the western U.S., Science, 339, 1572–1578, https://doi.org/10.1126/science.1227279, 2013.

Cziczo, D. J., Froyd, K. D., Hoose, C., Jensen, E. J., Diao, M., Zondlo, M. A., Smith, J. B., Twohy, C. H., and Murphy, D. M.: Clarifying the dominant sources and mechanisms of cirrus cloud formation., Science, 340, 1320–4, https://doi.org/10.1126/science.1234145, 2013.

Dee, D. P., Uppala, S. M., Simmons, A. J., Berrisford, P., Poli, P., Kobayashi, S., Andrae, U., Balmaseda, M. A., Balsamo, G., Bauer, P., Bechtold, P., Beljaars, A. C. M., van de Berg, L., Bidlot, J., Bormann, N., Delsol, C., Dragani, R., Fuentes, M., Geer, A. J., Haimberger, L., Healy, S. B., Hersbach, H., Hólm, E. V., Isaksen, L., Kållberg, P., Köhler, M., Matricardi, M., McNally, A. P., Monge-Sanz, B. M., Morcrette, J.-J., Park, B.-K., Peubey, C., de Rosnay, P., Tavolato, C., Thépaut, J.-N., and Vitart, F.: The ERA-Interim reanalysis: configuration and performance of the data assimilation system, Quarterly Journal of the Royal Meteorological Society, 137, 553–597, https://doi.org/10.1002/qj.828, 2011.

Delanoë, J., Protat, A., Testud, J., Bouniol, D., Heymsfield, A. J., Bansemer, A., Brown, P. R. A., Forbes, R. M., and Delanoë, J.: Statistical properties of the normalized ice particle size distribution, J. Geophys. Res., 110, https://doi.org/10.1029/2004JD005405, 2005.

Delanoë, J. and Hogan, R. J.: Combined CloudSat-CALIPSO-MODIS retrievals of the properties of ice clouds, J. Geophys. Res., 115, D00H29, https://doi.org/10.1029/2009JD012346, 2010.

Deng, M., Mace, G. G., Wang, Z., and Lawson, R. P.: Evaluation of Several A-Train Ice Cloud Retrieval Products with In Situ Measurements Collected during the SPARTICUS Campaign, J. App. Met. Clim., 52, 1014–1030, https://doi.org/10.1175/JAMC-D-12-054.1, 2013.

Field, P. R., Cotton, R. J., Johnson, D., Noone, K., Glantz, P., Kaye, P. H., Hirst, E., Greenaway, R. S., Jost, C., Gabriel, R., Reiner, T., Andreae, M., Saunders, C. P. R., Archer, A., Choularton, T., Smith, M., Brooks, B., Hoell, C., Bandy, B., and Heymsfield, A.: Ice nucleation in orographic wave clouds: Measurements made during INTACC, Q. J. R. Met. Soc., 127, 1493–1512, https://doi.org/10.1002/qj.49712757502, 2001.

Fusina, F., Spichtinger, P., and Lohmann, U.: Impact of ice supersaturated regions and thin cirrus on radiation in the midlatitudes, J. Geophys. Res, 112, https://doi.org/10.1029/2007JD008449, 2007.

Gasparini, B. and Lohmann, U.: Why cirrus cloud seeding cannot substantially cool the planet, J. Geophys. Res., 121, 4877–4893, https://doi.org/10.1002/2015JD024666, 2016.

Gayet, J.-F., Ovarlez, J., Shcherbakov, V., Ström, J., Schumann, U., Minikin, A., Auriol, F., Petzold, A., and Monier, M.: Cirrus cloud microphysical and optical properties at southern and northern midlatitudes during the INCA experiment, J. Geophys. Res., 109, D20 206, https://doi.org/10.1029/2004JD004803, 2004.

Ginoux, P., Prospero, J. M., Gill, T. E., Hsu, N. C., and Zhao, M.: Global-scale attribution of anthropogenic and natural dust sources and their emission rates based on MODIS Deep Blue aerosol products, Rev. Geophys., 50, 3005, https://doi.org/10.1029/2012RG000388, 2012.

Grawe, S., Augustin-Bauditz, S., Hartmann, S., Hellner, L., Pettersson, J. B. C., Prager, A., Stratmann, F., and Wex, H.: The immersion freezing behavior of ash particles from wood and brown coal burning, Atmos. Chem. Phys., 16, 13 911–13 928, https://doi.org/10.5194/acp-16-13911-2016, 2016.

Gryspeerdt, E., Quaas, J., and Bellouin, N.: Constraining the aerosol influence on cloud fraction, J. Geophys. Res., 121, 3566–3583, https://doi.org/10.1002/2015JD023744, 2016.

Gryspeerdt, E., Quaas, J., Ferrachat, S., Gettelman, A., Ghan, S., Lohmann, U., Morrison, H., Neubauer, D., Partridge, D. G., Stier, P., Takemura, T., Wang, H., Wang, M., and Zhang, K.: Constraining the instantaneous aerosol influence on cloud albedo, Proc. Nat. Acad. Sci. USA, 114, 4899–4904, https://doi.org/10.1073/pnas.1617765114, 2017a.

Gryspeerdt, E., Quaas, J., Goren, T., Klocke, D., and Brueck, M.: Technical note: An automated cirrus type classification, Atmos. Chem. Phys. Discuss., https://doi.org/10.5194/acp-2017-723, 2017b.

Heymsfield, A. J. and Miloshevich, L. M.: Homogeneous Ice Nucleation and Supercooled Liquid Water in Orographic Wave Clouds, J. Atmos. Sci., 50, 2335–2353, https://doi.org/10.1175/1520-0469(1993)050<2335:HINASL>2.0.CO;2, 1993.

Heymsfield, A. J., Krämer, M., Luebke, A., Brown, P., Cziczo, D. J., Franklin, C., Lawson, P., Lohmann, U., McFarquhar, G., Ulanowski, Z., and Van Tricht, K.: Cirrus Clouds, Met. Mono., 58, 2.1–2.26, https://doi.org/10.1175/AMSMONOGRAPHS-D-16-0010.1, 2017.

Heyn, I., Block, K., Mülmenstädt, J., Gryspeerdt, E., Kühne, P., and Quaas, J.: Assessment of simulated aerosol effective radiative forcings in the terrestrial spectrum, Geophys. Res. Lett, https://doi.org/10.1002/2016GL071975, 2017.

Hoose, C. and Möhler, O.: Heterogeneous ice nucleation on atmospheric aerosols: a review of results from laboratory experiments, Atmos. Chem. Phys., 12, 9817–9854, https://doi.org/10.5194/acp-12-9817-2012, 2012.

Hoyle, C. R., Luo, B. P., and Peter, T.: The Origin of High Ice Crystal Number Densities in Cirrus Clouds, J. Atmos. Sci., 62, 2568–2579, https://doi.org/10.1175/JAS3487.1, 2005.

Huang, Y., Siems, S. T., Manton, M. J., Protat, A., and Delanoë, J.: A study on the low-altitude clouds over the Southern Ocean using the DARDAR-MASK, J. Geophys. Res., 117, D18 204, https://doi.org/10.1029/2012JD017800, 2012.

Joos, H., Spichtinger, P., Lohmann, U., Gayet, J.-F., and Minikin, A.: Orographic cirrus in the global climate model ECHAM5, J. Geophys Res., 113, D18 205, https://doi.org/10.1029/2007JD009605, 2008.

Kanitz, T., Seifert, P., Ansmann, A., Engelmann, R., Althausen, D., Casiccia, C., and Rohwer, E. G.: Contrasting the impact of aerosols at northern and southern midlatitudes on heterogeneous ice formation, Geophys. Res. Lett., 38, L17 802, https://doi.org/10.1029/2011GL048532, 2011.

Kanji, Z. A., Ladino, L. A., Wex, H., Boose, Y., Burkert-Kohn, M., Cziczo, D. J., and Krämer, M.: Overview of Ice Nucleating Particles, Met. Mono., 58, 1.1–1.33, https://doi.org/10.1175/AMSMONOGRAPHS-D-16-0006.1, 2017.

Kärcher, B.: Cirrus Clouds and Their Response to Anthropogenic Activities, Curr. Clim. Ch. Rep., https://doi.org/10.1007/s40641-017-0060-3, 2017.

Kärcher, B. and Lohmann, U.: A parameterization of cirrus cloud formation: Heterogeneous freezing, J. Geophys. Res., 108, 4402, https://doi.org/10.1029/2002JD003220, 2003.

Kärcher, B. and Seifert, A.: On homogeneous ice formation in liquid clouds, Q. J. R. Met. Soc., 142, 1320–1334, https://doi.org/10.1002/qj.2735, 2016.

Kärcher, B. and Ström, J.: The roles of dynamical variability and aerosols in cirrus cloud formation, Atmos. Chem. Phys., 3, 823–838, https://doi.org/10.5194/acp-3-823-2003, 2003.

Kay, J. E. and Wood, R.: Timescale analysis of aerosol sensitivity during homogeneous freezing and implications for upper tropospheric water vapor budgets, Geophys. Res. Lett., 35, L10 809, https://doi.org/10.1029/2007GL032628, 2008.

Kojima, T., Buseck, P. R., Wilson, J. C., Reeves, J. M., and Mahoney, M. J.: Aerosol particles from tropical convective systems: Cloud tops and cirrus anvils, J. Geophys. Res., 109, D12 201, https://doi.org/10.1029/2003JD004504, 2004.

Koop, T., Luo, B., Tsias, A., and Peter, T.: Water activity as the determinant for homogeneous ice nucleation in aqueous solutions, Nature, 406, 611–614, https://doi.org/10.1038/35020537, 2000.

Korolev, A. V., Emery, E. F., Strapp, J. W., Cober, S. G., and Isaac, G. A.: Quantification of the Effects of Shattering on Airborne Ice Particle Measurements, J. Atmos. Ocean. Tech., 30, 2527–2553, https://doi.org/10.1175/JTECH-D-13-00115.1, 2013.

Krämer, M., Schiller, C., Afchine, A., Bauer, R., Gensch, I., Mangold, A., Schlicht, S., Spelten, N., Sitnikov, N., Borrmann, S., de Reus, M., and Spichtinger, P.: Ice supersaturations and cirrus cloud crystal numbers, Atmos. Chem. Phys., 9, 3505–3522, https://doi.org/10.5194/acp-9-3505-2009, 2009.

Krämer, M., Rolf, C., Luebke, A., Afchine, A., Spelten, N., Costa, A., Meyer, J., Zöger, M., Smith, J., Herman, R. L., Buchholz, B., Ebert, V., Baumgardner, D., Borrmann, S., Klingebiel, M., and Avallone, L.: A microphysics guide to cirrus clouds – Part 1: Cirrus types, Atmos. Chem. Phys., 16, 3463–3483, https://doi.org/10.5194/acp-16-3463-2016, 2016.

Lindsey, D. T. and Fromm, M.: Evidence of the cloud lifetime effect from wildfire-induced thunderstorms, Geophys. Res. Lett., 35, https://doi.org/10.1029/2008GL035680, 2008.

Liou, K.-N.: Influence of Cirrus Clouds on Weather and Climate Processes: A Global Perspective, Mon. Weather Rev., 114, 1167–1199, https://doi.org/10.1175/1520-0493(1986)114<1167:IOCCOW>2.0.CO;2, 1986.

Lohmann, U. and Kärcher, B.: First interactive simulations of cirrus clouds formed by homogeneous freezing in the ECHAM general circulation model, J. Geophys. Res., 107, https://doi.org/10.1029/2001JD000767, 2002.

Lohmann, U., Stier, P., Hoose, C., Ferrachat, S., Kloster, S., Roeckner, E., and Zhang, J.: Cloud microphysics and aerosol indirect effects in the global climate model ECHAM5-HAM, Atmos. Chem. Phys., 7, 3425, 2007.

Luebke, A. E., Afchine, A., Costa, A., Grooß, J.-U., Meyer, J., Rolf, C., Spelten, N., Avallone, L. M., Baumgardner, D., and Krämer, M.: The origin of midlatitude ice clouds and the resulting influence on their microphysical properties, Atmos. Chem. Phys., 16, 5793–5809, https://doi.org/10.5194/acp-16-5793-2016, 2016.

Mamouri, R.-E. and Ansmann, A.: Potential of polarization lidar to provide profiles of CCN- and INP-relevant aerosol parameters, Atmos. Chem. Phys., 16, 5905–5931, https://doi.org/10.5194/acp-16-5905-2016, 2016.

Möhler, O., Field, P. R., Connolly, P., Benz, S., Saathoff, H., Schnaiter, M., Wagner, R., Cotton, R., Krämer, M., Mangold, A., and Heymsfield, A. J.: Efficiency of the deposition mode ice nucleation on mineral dust particles, Atmos. Chem. Phys., 6, 3007–3021, https://doi.org/10.5194/acp-6-3007-2006, 2006.

Morcrette, J.-J., Boucher, O., Jones, L., Salmond, D., Bechtold, P., Beljaars, A., Benedetti, A., Bonet, A., Kaiser, J. W., Razinger, M., Schulz, M., Serrar, S., Simmons, A. J., Sofiev, M., Suttie, M., Tompkins, A. M., and Untch, A.: Aerosol analysis and forecast in the European Centre for Medium-Range Weather Forecasts Integrated Forecast System: Forward modeling, Journal of Geophysical Research: Atmospheres, 114, D06 206, https://doi.org/10.1029/2008JD011235, 2009.

Muhlbauer, A., Ackerman, T. P., Comstock, J. M., Diskin, G. S., Evans, S. M., Lawson, R. P., and Marchand, R. T.: Impact of large-scale dynamics on the microphysical properties of midlatitude cirrus, J Geophys. Res., 119, 3976–3996, https://doi.org/10.1002/2013JD020035, 2014.

O'Shea, S. J., Choularton, T. W., Lloyd, G., Crosier, J., Bower, K. N., Gallagher, M., Abel, S. J., Cotton, R. J., Brown, P. R. A., Fugal, J. P., Schlenczek, O., Borrmann, S., and Pickering, J. C.: Airborne observations of the microphysical structure of two contrasting cirrus clouds, J. Geophys. Res., 121, 13, https://doi.org/10.1002/2016JD025278, 2016.

Platnick, S., Meyer, K. G., King, M. D., Wind, G., Amarasinghe, N., Marchant, B., Arnold, G. T., Zhang, Z., Hubanks, P. A., Holz, R. E., Yang, P., Ridgway, W. L., and Riedi, J.: The MODIS Cloud Optical and Microphysical Products: Collection 6 Updates and Examples From Terra and Aqua, IEEE Trans. Geosci. Remote Sens., 55, 502–525, https://doi.org/10.1109/TGRS.2016.2610522, 2017.

Pruppacher, H. R. and Klett, J. D.: Microphysics of Clouds and Precipitation, Kluwer Acad., Norwell, Mass., 1997.

Quaas, J., Ming, Y., Menon, S., Takemura, T., Wang, M., Penner, J., Gettelman, A., Lohmann, U., Bellouin, N., Boucher, O., Sayer, A., Thomas, G., McComiskey, A., Feingold, G., Hoose, C., Kristjánsson, J., Liu, X., Balkanski, Y., Donner, L., Ginoux, P., Stier, P., Grandey, B., Feichter, J., Sednev, I., Bauer, S., Koch, D., Grainger, R., Kirkevåg, A., Iversen, T., Seland, Ø., Easter, R., Ghan, S., Rasch, P., Morrison, H., Lamarque, J.-F., Iacono, M., Kinne, S., and Schulz, M.: Aerosol indirect effects - general circulation model intercomparison and evaluation with satellite data, Atmos. Chem. Phys., 9, 8697–8717, https://doi.org/10.5194/acp-9-8697-2009, 2009.

Rosenfeld, D., Yu, X., Liu, G., Xu, X., Zhu, Y., Yue, Z., Dai, J., Dong, Z., Dong, Y., and Peng, Y.: Glaciation temperatures of convective clouds ingesting desert dust, air pollution and smoke from forest fires, Geophys. Res. Lett., 38, 21 804, https://doi.org/10.1029/2011GL049423, 2011.

Salzmann, M., Ming, Y., Golaz, J.-C., Ginoux, P. A., Morrison, H., Gettelman, A., Krämer, M., and Donner, L. J.: Two-moment bulk stratiform cloud microphysics in the GFDL AM3 GCM: description, evaluation, and sensitivity tests, Atmos. Chem. Phys., 10, 8037–8064, https://doi.org/10.5194/acp-10-8037-2010, 2010.

Seifert, A., Heus, T., Pincus, R., and Stevens, B.: Large-eddy simulation of the transient and near-equilibrium behavior of precipitating shallow convection, J. Adv. Mod. Earth Sys., https://doi.org/10.1002/2015MS000489, 2015.

Sourdeval, O., Gryspeerdt, E., Krämer, M., Goren, T., Delanoë, J., Afchine, A., Hemmer, F., and Quaas, J.: Ice crystal number concentration estimates from lidar-radar satellite remote sensing. Part 1: Method and evaluation, Atmos. Chem. Phys. Discuss., submitted.

Stephens, G. L., Li, J., Wild, M., Clayson, C. A., Loeb, N., Kato, S., L'Ecuyer, T., Stackhouse, P. W., Lebsock, M., and Andrews, T.: An update on Earth's energy balance in light of the latest global observations, Nat. GeoSci., 5, 691–696, https://doi.org/10.1038/NGEO1580, 2012.

Tan, I., Storelvmo, T., and Choi, Y.-S.: Spaceborne lidar observations of the ice-nucleating potential of dust, polluted dust, and smoke aerosols in mixed-phase clouds, J. Geophys. Res., 119, 6653–6665, https://doi.org/10.1002/2013JD021333, 2014.

Weigum, N. M., Stier, P., Schwarz, J. P., Fahey, D. W., and Spackman, J. R.: Scales of variability of black carbon plumes over the Pacific Ocean, 39, L15 804, https://doi.org/10.1029/2012GL052127, 2012.

Wernli, H., Boettcher, M., Joos, H., Miltenberger, A. K., and Spichtinger, P.: A trajectory-based classification of ERA-Interim ice clouds in the region of the North Atlantic storm track, Geophys. Res. Lett., https://doi.org/10.1002/2016GL068922, 2016.

Zhang, D., Wang, Z., Heymsfield, A., Fan, J., Liu, D., and Zhao, M.: Quantifying the impact of dust on heterogeneous ice generation in midlevel supercooled stratiform clouds, Geophys. Res. Lett., 39, https://doi.org/10.1029/2012GL052831, 2012.